Eur. Phys. J. C 11, 309–316 (1999)
Digital Object Identifier (DOI) 10.1007/s100529900182

THE EUROPEAN PHYSICAL JOURNAL C

Spin effects in diffractive J/Ψ leptoproduction and the structure of Pomeron coupling

S.V. Goloskokov

Bogoliubov Laboratory of Theoretical Physics, Joint Institute for Nuclear Research, 141980 Dubna, Moscow region, Russia

Received: 27 April 1999 / Revised version: 29 June 1999 / Published online: 14 October 1999

Abstract. We calculate the cross section and A_{ll} asymmetry of the diffractive J/Ψ leptoproduction for a simple model of a Pomeron coupling with a proton, which contains the γ^α term and a spin-dependent part. It is shown that the asymmetry caused by the Pomeron coupling $\propto \gamma^\alpha$ does not vanish for nonzero $|t|$. The sensitivity of the polarized diffractive J/Ψ production to the spin-dependent part of the Pomeron coupling is found to be rather weak. As a result, it is difficult to study the structure of the Pomeron coupling with the proton in future polarized diffractive experiments on the J/Ψ production.

1 Introduction

The study of diffractive processes at HERA has renewed interest in investigating the nature of the Pomeron. New results on the Pomeron intercept in diffractive events and information about the Pomeron partonic structure have been obtained in H1 and ZEUS experiments [1,2]. Among different diffractive processes, which have been studied experimentally at DESY, vector-meson production [3,4] has a key place. These reactions can give information on the gluon distribution in the nucleon at small x and on the structure of the Pomeron. The diffractive J/Ψ production has a significant role in these investigations. In contrast with the ρ meson production, the $q\bar{q}$ exchange in the t channel is not important here and the predominant contribution is determined by a color-singlet t-channel exchange (Pomeron).

The phenomenological Pomeron describes the cross section of elastic reactions at high energies and the low-x behavior of the structure functions. From the fit of soft elastic processes, the linear soft Pomeron trajectory [5]

$$\alpha_p(t) = 1 + \epsilon^s + \alpha' t, \tag{1}$$

was suggested, with $\epsilon^s = 0.08$ and $\alpha' = 0.25$ GeV^{-2}. However, the value $\alpha_p(0)$ =1.12–1.2 of the Pomeron intercept, which has been obtained at HERA [2], is inconsistent with the soft Pomeron with $\epsilon^s = 0.08$. The explanation of this discrepancy may be quite simple. In the soft reactions, the interaction time is large and the Pomeron rescattering effects must be important. It has been found in [6] that the rescattering effects decrease the value of the Pomeron intercept from $\epsilon \sim 0.15$ for the hard "bare" Pomeron to $\epsilon \sim 0.08$ for the soft Pomeron. Thus, in hard diffractive processes like the J/Ψ production, the value of ϵ should be about 0.15.

Different models of the Pomeron [7] have been used to study the diffractive vector-meson production [8–11]. The models [8,9], based on the dominant role of the Pomeron contribution in these processes, reproduce the main features of the vector-meson production: the mass, Q^2, t, and energy dependencies of the cross section. In the QCD-inspired models, the Pomeron is modeled by two gluons [12]. It is usually assumed that the Pomeron couples to a proton, for example like a $C = +1$ isoscalar photon [13], and has a simple γ^α vertex. A more general form of the Pomeron coupling, an isoscalar nucleon current with isoscalar Dirac and Pauli form factors, has been used in [14,15] to study the diffractive processes. In these approaches, the cross sections are dependent on the Pomeron coupling with the proton. Otherwise, it has been found in [10,11] that the cross section of the vector-meson photoproduction in the forward limit $|t| = 0$ and high Q^2 is proportional to $[xG(x,\bar{Q}^2)]^2$. The typical scale here is determined by $\bar{Q}^2 = (Q^2 + M_V^2)/4$ [10,11] where Q^2 is the photon virtuality and M_V is the mass of the vector meson. For the diffractive J/Ψ production, the scale is large enough even for small Q^2, and perturbative calculations can be used. We see that the cross sections of diffractive reactions are expressed, on one hand, in terms of the Pomeron coupling, and on the other hand, through gluon distributions. Consequently, these quantities should be related.

The sensitivity of diffractive lepto- and photoproduction to the gluon density in the proton can give an excellent tool to test $G(x)$ [10]. The relation of the spin-average diffractive production with the gluon structure function of the proton gives way to an assumption that the longitudinal double-spin asymmetry in such processes might be proportional to $[\Delta G/G]$ [16]. Contrary to those results, it has been found in [17] that the A_{ll} asymmetry in the diffractive vector-meson production should be zero for $|t| = 0$. As a result, this process cannot be used to study ΔG of the proton.

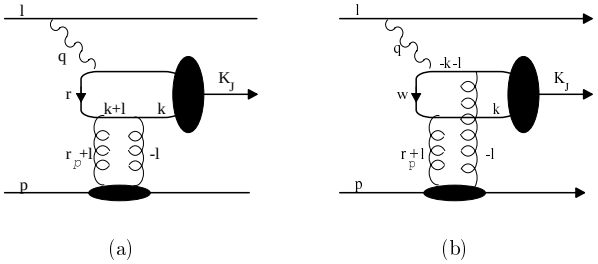

Fig. 1a,b. Feynman graphs for the diffractive vector-meson production

The value of the asymmetry in the polarized vector-meson production in diffractive processes for nonzero $|t|$ is not well known now. It is very important to perform model calculations of spin-dependent J/Ψ leptoproduction to obtain quantitative estimations of spin asymmetries and their connection with the Pomeron coupling structure (see [18]). In this paper, we calculate the cross section and the $A_{\rm ll}$ asymmetry of the diffractive J/Ψ leptoproduction. The cross section of the J/Ψ leptoproduction can be decomposed into the leptonic and hadronic tensors, the amplitude of the $\gamma^\star\mathbf{P} \to$ J/Ψ transition, and the Pomeron exchange. After describing some kinematics of the process in Sect. 2, we consider the structure of the leptonic and hadronic tensors in Sect. 3. We use a simple form of the proton coupling with the two-gluon system that is similar to those introduced in [14]. In Sect. 4, we calculate the spin-dependent cross section of the J/Ψ leptoproduction for the longitudinal polarization of the initial lepton and proton. The numerical results for the diffractive J/Ψ production at HERA and HERMES energies is presented in Sect. 5. We finish with concluding remarks in Sect. 6.

2 Kinematics of diffractive J/Ψ leptoproduction

Let us study the diffractive J/Ψ production

$$l + p \to l + p + \mathrm{J}/\Psi \tag{2}$$

at high energies $s = (p+l)^2$ and fixed momentum transfer $t = r_{\rm P}^2 = (p-p')^2$. Here p and l are the initial momenta of the lepton and proton, p' is the final proton momentum and $r_{\rm P}$ is a momentum carried by the Pomeron. The graphs, which describe reaction 2, are shown in Fig. 1a,b. The gluons from the Pomeron are coupled with single and different quarks in the $c\bar{c}$ loop. This ensures the gauge invariance of the final result [19]. The blob in the proton line represents the proton–two-gluon coupling which comprises the high-energy t-channel gluon ladder of the Pomeron except the simple two-gluon exchange. The reaction (2) is described by, in addition to s and t, the variables

$$Q^2 = -q^2, \quad y = \frac{p\cdot q}{p\cdot l}, \quad x_{\rm P} = \frac{q\cdot r_{\rm P}}{q\cdot p}, \tag{3}$$

where Q^2 is the photon virtuality.

The light-cone variables convenient for our calculations are determined by $a_\pm = a_0 \pm a_z$. In these variables, the scalar product of two four-vectors looks like

$$a\cdot b = \frac{1}{2}(a_+ b_- + a_- b_+) - \mathbf{a}_\perp \mathbf{b}_\perp,$$

where $\mathbf{a}_\perp$ and $\mathbf{b}_\perp$ represent the transverse parts of the momenta. We use the center-of-mass system, where the momenta of the initial lepton and proton are going along the z axis and have the form

$$l = \left(p_+, \frac{\mu^2}{p_+}, \mathbf{0}\right), \quad p = \left(\frac{m^2}{p_+}, p_+, \mathbf{0}\right). \tag{4}$$

Here μ and m are the lepton and proton mass. The energy of the lepton–proton system then reads as $s \sim p_+^2$. We can determine the spin vectors with positive helicity of the lepton and the proton by

$$s_{\rm l} = \frac{1}{\mu}\left(p_+, -\frac{\mu^2}{p_+}, \mathbf{0}\right), \quad s_{\rm l}^2 = -1, \quad s_{\rm l}\cdot l = 0;$$
$$s_{\rm p} = \frac{1}{m}\left(-\frac{m^2}{p_+}, p_+, \mathbf{0}\right), \quad s_{\rm p}^2 = -1, \quad s_{\rm p}\cdot p = 0. \tag{5}$$

The momenta are carried by the photon and the Pomeron, and can be written as follows:

$$q = \left(yp_+, -\frac{Q^2}{p_+}, \mathbf{q}_\perp\right), \quad |q_\perp| = \sqrt{Q^2(1-y)}, \quad q^2 = -Q^2;$$
$$r_{\rm P} = \left(-\frac{|t|}{p_+}, x_{\rm P}p_+, \mathbf{r}_\perp\right), \quad |r_\perp| = \sqrt{|t|(1-x_{\rm P})}, \quad r_{\rm P}^2 = t. \tag{6}$$

Thus, y and $x_{\rm P}$ are the fractions of the longitudinal momenta of the lepton and proton carried by the photon and Pomeron, respectively. From the mass-shell equation for vector-meson momentum $K_{\rm J}^2 = (q + r_{\rm P})^2 = M_{\rm J}^2$, we find that, for these reactions,

$$x_{\rm P} \sim \frac{m_{\rm J}^2 + Q^2 + |t|}{sy} \tag{7}$$

and that $x_{\rm p}$ is small at high energies.

3 Structure of leptonic and hadronic tensors

3.1 Leptonic tensor

The structure of the leptonic tensor is quite simple [21] because the lepton is a point-like object

$$\mathcal{L}^{\mu\nu}(s_{\rm l}) = \sum_{\rm spin\ s_f} \bar{u}(l', s_{\rm f})\gamma^\mu u(l, s_{\rm l})\bar{u}(l, s_{\rm l})\gamma^\nu u(l', s_{\rm f})$$
$$= \mathrm{Tr}\left[(\not{l}' + \mu)\frac{1+\gamma_5 \not{s}_{\rm l}}{2}\gamma^\nu(\not{l} + \mu)\gamma^\mu\right]. \tag{8}$$

Here l and l' are the initial and final lepton momenta, and $s_{\rm l}$ is a spin vector of the initial lepton determined in (5).

The sum and difference of the cross sections with parallel and antiparallel longitudinal polarization of a proton and a lepton are expressed in terms of the spin-average and spin-dependent hadron and lepton tensors

$$\mathcal{L}^{\mu\nu}(\pm) = \frac{1}{2}\left(\mathcal{L}^{\mu\nu}\left(+\frac{1}{2}\right) \pm \mathcal{L}^{\mu\nu}\left(-\frac{1}{2}\right)\right), \qquad (9)$$

where $\mathcal{L}^{\mu\nu}(\pm\frac{1}{2})$ are the tensors with the helicity of the initial lepton equal to $\pm 1/2$. The tensors (9) look like

$$\begin{aligned}\mathcal{L}^{\mu\nu}(+) &= 2(g^{\mu\nu} l\cdot q + 2l^\mu l^\nu - l^\mu q^\nu - l^\nu q^\mu),\\ \mathcal{L}^{\mu\nu}(-) &= 2\mathrm{i}\mu\epsilon^{\mu\nu\delta\rho} q_\delta (s_l)_\rho. \end{aligned} \qquad (10)$$

3.2 Pomeron–proton coupling

The Pomeron is a vacuum t-channel exchange that describes diffractive processes at high energies. The Pomeron contribution to the hadron–hadron scattering amplitude can be written in the form

$$T(s,t) = \mathrm{i}\boldsymbol{P}(s,t) V_{\mathrm{AP}} \otimes V_{\mathrm{BP}}, \qquad (11)$$

where $\boldsymbol{P}$ is a function determined by the Pomeron and V_{AP} and V^{BP} are the Pomeron couplings with particles A and B, respectively.

The spin structure of the Pomeron coupling is an open problem now. When the gluons from the Pomeron couple to a single quark in the hadron, a simple matrix structure of the Pomeron vertex

$$V^{\alpha}_{\mathrm{hP}} = B_{\mathrm{hP}}\gamma^\alpha \qquad (12)$$

appears in a QCD-based model [20]. This γ^α coupling leads to transverse spin-flip effects decreasing with increasing energy as $1/s$. The effective Pomeron coupling with the hadron (12) is like a $C = +1$ isoscalar photon vertex [13]. Then, the Pomeron–proton coupling should be equivalent to the isoscalar electromagnetic nucleon current. The spin-dependent Pomeron coupling can be obtained if one considers together with the Dirac form factor (12) the Pauli form factor [14] in the electromagnetic nucleon current. If the gluons from the Pomeron carry some fraction x_{P} of the initial proton momenta, this coupling can be written in the form

$$V^{\alpha}_{\mathrm{pgg}}(p,t,x_{\mathrm{P}}) = 2p^\alpha A(t,x_{\mathrm{P}}) + \gamma^\alpha B(t,x_{\mathrm{P}}). \qquad (13)$$

Let us study the meson–nucleon scattering described at high energies and the fixed momentum transfer by the Pomeron contribution. The coupling of the Pomeron with the meson for small $|t|$ can be written in the form $q^\mu\phi(t)$, where q is the initial meson four-momentum and $\phi(t)$ is a meson–Pomeron form factor. This form is similar to the photon–meson vertex. For the Pomeron–proton coupling (13), we find the following meson–nucleon scattering amplitude:

$$M(\tilde{s},t) = \mathrm{i}\left[\tilde{s}A(t,x_{\mathrm{P}}) + \not{q}B(t,x_{\mathrm{P}})\right]\phi(t). \qquad (14)$$

Here $\tilde{s} = (p+q)^2$ and $x_{\mathrm{P}} \propto 1/\tilde{s}$. Thus, the Pomeron coupling (13) provides the standard form of the scattering amplitude. The meson–proton helicity-nonflip and helicity-flip amplitudes are expressed in terms of the invariant functions A and B:

$$\begin{aligned}F_{++}(s,t) &= \mathrm{i}\tilde{s}[B(t,x_{\mathrm{P}}) + 2mA(t,x_{\mathrm{P}})]\phi(t);\\ F_{+-}(s,t) &= \mathrm{i}\tilde{s}\sqrt{|t|}A(t,x_{\mathrm{P}})\phi(t),\end{aligned} \qquad (15)$$

and the spin-average cross-section is written in the form

$$\frac{\mathrm{d}\sigma}{\mathrm{d}t} \sim [|B+2mA|^2 + |t||A|^2]\phi(t)^2. \qquad (16)$$

Here m is a proton mass. We see that the term proportional to B represents the Pomeron coupling that leads to the nonflip amplitude. The A function is the spin-dependent part of the Pomeron coupling, which produces spin-flip effects that are nonvanishing at high-energies. The absolute value of the ratio of A to B is proportional to the ratio of helicity-flip and -nonflip amplitudes. It has been found in [22,23] that the ratio $|A|/|B|$ is about 0.1–0.2 GeV^{-1} and has a weak energy dependence. This value of the $|A|/|B|$ ratio and weak energy dependence of spin asymmetries in exclusive reactions is not in contradiction with the experiment [24] and is confirmed by the model results (see [22,25], for example).

A proton–Pomeron coupling similar to (13) has been used in [15] to analyze the spin effects in diffractive vector-meson production. In the model [22], the form (13) was found to be valid for small momentum transfer $|t| <$ few GeV^2 and the $A(t)$ function to be caused by the meson-cloud effects in the nucleon. This model gives a quantitative description of meson–nucleon and nucleon–nucleon polarized scattering at high energies. The complicated spin structure of the Pomeron coupling may be due to the nonperturbative structure of the proton. In a QCD-based model, in which the proton is viewed as being composed of a quark and a diquark [26], the structure (13) for the proton coupling with a two-gluon system has been found for moderate momentum transfer [23]. The $A(t)$ contribution is determined there by the effects of vector diquarks inside the proton, which are of the order of α_s. In all the cases, the spin-flip $A(t)$ contribution is determined by the nonperturbative effects in the proton.

Since the Pomeron consists of two gluons [12], the Pomeron coupling should have two gluon indices. We use in calculations the following generalization of (13) as an ansatz:

$$\begin{aligned}V^{\alpha\alpha'}_{\mathrm{pgg}}(p,t,x_{\mathrm{P}},l) &= 4p^\alpha p^{\alpha'} A(t,x_{\mathrm{P}},l)\\ &\quad + (\gamma^\alpha p^{\alpha'} + \gamma^{\alpha'} p^\alpha) B(t,x_{\mathrm{P}},l).\end{aligned} \qquad (17)$$

This vertex is shown in Fig. 1a,b by the blob in the proton line. The properties of the structure (17) are completely equivalent to the coupling (13) (see Sect. 3.3 and 3.4). It has been mentioned above that this vertex contains the gluon ladder, except for two gluons that provide the l dependencies in (17). In what follows, we shall calculate the imaginary part of the Pomeron contribution to the scattering amplitude, which dominates in the high-energy region.

This contribution is equivalent to the t-channel cut in the gluon-loop graph.

3.3 Simple form of hadronic tensor

The hadronic tensor for the vertex (13) can be written in the form

$$W^{\alpha;\beta}(s_{\rm p}) = \sum_{\text{spin } s_{\rm f}} \bar{u}(p',s_{\rm f})V^{\alpha}_{\rm pgg}(p,t,x_{\rm P})u(p,s_{\rm p})\cdot \bar{u}(p,s_{\rm p})V^{\beta\,+}_{\rm pgg}(p,t,x_{\rm P})u(p',s_{\rm f}). \quad (18)$$

Here p and p' are the initial and final proton momenta and $s_{\rm p}$ is a spin vector of the initial proton. The spin-average and spin-dependent hadron tensors are determined similarly as in (9). The leading term of the spin-average hadron tensor must have a maximum number of the large proton momenta p^{α}. It looks like

$$W^{\alpha;\beta}(+) = 4p^{\alpha}p^{\beta}(|B+2mA|^2+|t||A|^2) \quad (19)$$

and is proportional to the meson–proton cross section (16) up to some function of t.

The spin-dependent part of the hadron tensor can be represented as a sum of structures which have different natures:

$$W^{\alpha;\beta}(-) = \Delta A^{\alpha;\beta}_{\gamma} + \Delta A^{\alpha;\beta}_{1}. \quad (20)$$

The ΔA_{γ} term has indices of different Pomeron couplings in the ϵ function

$$\Delta A^{\alpha;\beta}_{\gamma} = 2{\rm i}m|B|^2\epsilon^{\alpha\beta\gamma\delta}(r_{\rm P})_{\gamma}(s_{\rm p})_{\delta}. \quad (21)$$

This contribution is proportional to $|B|^2$ and equivalent in form to the spin-dependent part of the leptonic tensor (see (10)); we call it a γ-coupling asymmetry. The ΔA_1 term contains both A and B amplitudes from (13):

$$\Delta A^{\alpha;\beta}_{1} = \left[4p^{\beta}B\right]\left[2{\rm i}A^{\star}\epsilon^{\alpha\gamma\delta\rho}p_{\gamma}(r_{\rm P})_{\delta}(s_{\rm p})_{\rho}\right] - \left[4p^{\alpha}B^{\star}\right]\left[2{\rm i}A\epsilon^{\beta\gamma\delta\rho}p_{\gamma}(r_{\rm P})_{\delta}(s_{\rm p})_{\rho}\right]. \quad (22)$$

3.4 Generalized hadronic tensor

The hadronic tensor for the ansatz (17) is given by

$$W^{\alpha\alpha';\beta\beta'}(s_{\rm p}) = \sum_{\text{spin } s_{\rm f}} \bar{u}(p',s_{\rm f})V^{\alpha\alpha'}_{\rm pgg}(p,t,x_{\rm P},l)u(p,s_{\rm p})\cdot \bar{u}(p,s_{\rm p})V^{\beta\beta'\,+}_{\rm pgg}(p,t,x_{\rm P},l')u(p',s_{\rm f}). \quad (23)$$

The spin-average and spin-dependent hadron tensors are written as

$$W^{\alpha\alpha';\beta\beta'}(\pm) = \frac{1}{2}\left(W^{\alpha\alpha';\beta\beta'}\left(+\frac{1}{2}\right) \pm W^{\alpha\alpha';\beta\beta'}\left(-\frac{1}{2}\right)\right). \quad (24)$$

For the leading term of $W(+)$, we find

$$W^{\alpha\alpha';\beta\beta'}(+) = 16p^{\alpha}p^{\alpha'}p^{\beta}p^{\beta'}(|B+2mA|^2+|t||A|^2). \quad (25)$$

Note that we omit for simplicity here and in what follows the arguments of the A and B functions unless it is necessary. However, we shall remember that the amplitudes A and B depend on l, otherwise the complex conjugative values $A^{\star}$ and $B^{\star}$ are functions of l'.

The spin-dependent part of the hadron tensor can be written as

$$W^{\alpha\alpha';\beta\beta'}(-) = \Delta A^{\alpha\alpha';\beta\beta'}_{\gamma} + \Delta A^{\alpha\alpha';\beta\beta'}_{1}. \quad (26)$$

Here

$$\Delta A^{\alpha\alpha';\beta\beta'}_{\gamma} = 2{\rm i}m|B|^2\cdot \left[p^{\alpha'}p^{\beta'}\epsilon^{\alpha\beta\gamma\delta}(r_{\rm P})_{\gamma}(s_{\rm p})_{\delta} + \binom{\text{all per-}}{\text{mutations}}\binom{\{\alpha\to\alpha'\}}{\{\beta\to\beta'\}}\right] \quad (27)$$

and

$$\Delta A^{\alpha\alpha';\beta\beta'}_{1} = \left[4p^{\beta}p^{\beta'}B\right]\left[2{\rm i}A^{\star}p^{\alpha'}\epsilon^{\alpha\gamma\delta\rho}p_{\gamma}(r_{\rm P})_{\delta}(s_{\rm p})_{\rho} + \{\alpha\to\alpha'\}\right] - \left[4p^{\alpha}p^{\alpha'}B^{\star}\right]\left[2{\rm i}Ap^{\beta'}\epsilon^{\beta\gamma\delta\rho}p_{\gamma}(r_{\rm P})_{\delta}(s_{\rm p})_{\rho} + \{\beta\to\beta'\}\right]. \quad (28)$$

The ΔA_1 term has the form of a product of the spin-dependent part ΔA of one proton vertex and the symmetric part S of the other. It can be written as

$$\Delta A_1 = -(\Delta A^{\alpha\alpha'})^{\star}S^{\beta\beta'} - \Delta A^{\beta\beta'}(S^{\alpha\alpha'})^{\star}, \quad (29)$$

where

$$S^{\beta\beta'} = \left[4Bp^{\beta}p^{\beta'}\right];$$
$$\Delta A^{\alpha\alpha'} = \left[2{\rm i}Ap^{\alpha'}\epsilon^{\alpha\gamma\delta\rho}p_{\gamma}(r_{\rm P})_{\delta}(s_{\rm p})_{\rho} + \{\alpha\to\alpha'\}\right]. \quad (30)$$

We see that ΔA_{γ} and ΔA_1 from (26), in contrast with the relevant terms in (20), have the additional $p^{\alpha'}p^{\beta'}$ momenta and symmetrization over $\alpha\to\alpha'$, $\beta\to\beta'$ indices. The powers of large scalar production $p\cdot q$ which appear in this case will be compensated after the loop integration over l and l'. As a result, (20) and (26) will produce the same spin-dependent amplitude. Using the above-mentioned argument, we find that the forms (19) and (25) lead to the same spin-average amplitude. Hence, the Pomeron couplings (13) and (17) are equivalent. The very important property of (20,26) is that both the B^2 and $A\cdot B$ terms contribute to the $W(-)$ tensor, which is responsible for the asymmetry.

4 Diffractive J/Ψ leptoproduction

4.1 Amplitude of the $\gamma\mathbb{P}\to$ J/Ψ transition

Now we address the structure of the amplitude of $\gamma\mathbb{P}\to$ J/Ψ production. In what follows, we have regarded the J/Ψ meson as an S-wave system of $c\bar{c}$ quarks [27]. The J/Ψ wave function in this case has the form $g(\not{k}+m_{\rm c})\gamma_{\mu}$, where k is the quark momentum and $m_{\rm c}$ is its mass. In the nonrelativistic approximation, both the quarks have

the same momentum k, equal to half of the vector-meson momentum $K_{\rm J}$, and the mass of the c quark is equal to $m_{\rm J}/2$. The coupling constant g can be expressed through the e^+e^- decay width of the J/Ψ meson

$$g^2 = \frac{3\Gamma^{\rm J}_{e^+e^-} m_{\rm J}}{64\pi\alpha^2}. \quad (31)$$

The gluons from the Pomeron are coupled with the single and different quarks in the $c\bar{c}$ loop (see Fig. 1a, b). The $\gamma\mathbf{P} \to {\rm J}/\Psi$ transition amplitudes for these graphs look like

$$T_{\rm a} = g{\rm Tr}[\not e_{\rm J}(\not k + m_{\rm c})\gamma_\alpha(\not k + \not l + m_{\rm c})\gamma_{\alpha'}(\not r + m_{\rm c})\gamma_\nu] \times \frac{1}{r^2 - m_{\rm c}^2};$$
$$T_{\rm b} = g{\rm Tr}[\not e_{\rm J}(\not k + m_{\rm c})\gamma_{\alpha'}(\not w + m_{\rm c})\gamma_\nu(-\not k - \not l + m_{\rm c})\gamma_\alpha] \times \frac{1}{w^2 - m_{\rm c}^2}. \quad (32)$$

Here $r = k - r_{\rm P}$ and $w = k - r_{\rm P} - l$ are the momenta of the off-mass shell quark in the loop for the diagram, Fig.1. a, b, respectively, and $e_{\rm J}$ is polarization of the J/Ψ meson, which obeys the relation

$$\sum_{\rm spin_J} e^\rho_{\rm J}(e^\sigma_{\rm J})^+ = -g^{\rho\sigma} + \frac{K^\rho_{\rm J} K^\sigma_{\rm J}}{m^2_{\rm J}}. \quad (33)$$

It is known (see [10,11], for example) that the leading terms of the amplitude of the diffractive vector-meson production are mainly imaginary. To calculate the imaginary part, we must consider the δ-function contribution in the s-channel propagators ($k + l$ and $p' - l$ lines for Fig. 1a). With the help of these δ functions, the integration over l,

$$\int {\rm d}^4 l = \frac{1}{2}\int {\rm d}l_+ {\rm d}l_- {\rm d}l_\perp \quad (34)$$

can be carried out over l_+ and l_- variables. One can find that both the $l_\pm$ components of the vector l are small: $l_+ \sim l_- \propto 1/p_+$. This results in the transversity of the gluon momentum $l^2 \simeq -l^2_\perp$. The same is true for integration over l in the nonplanar graph of Fig. 1b. For the arguments in the propagator of graphs, Fig. 1a,b, we find

$$r^2 - m_{\rm c}^2 = -\frac{M^2_{\rm J} + Q^2 + |t|}{2},$$
$$w^2 - m_{\rm c}^2 = -2\left(l^2_\perp + \mathbf{l}_\perp \mathbf{r}_\perp + \frac{M^2_{\rm J} + Q^2 + |t|}{4}\right). \quad (35)$$

Thus these quark lines are far from the mass shell for heavy vector-meson production even for small Q^2 [10].

4.2 Cross section of vector meson production

The spin-average and spin-dependent cross sections with parallel and antiparallel longitudinal polarization of a lepton and a proton are determined by the relation

$$\sigma(\pm) = \frac{1}{2}\left(\sigma(\overrightarrow{\Leftarrow}) \pm \sigma(\overrightarrow{\Rightarrow})\right). \quad (36)$$

These cross sections are expressed through the squared amplitude of the $\gamma\mathbf{P} \to {\rm J}/\Psi$ transition and convoluted with the spin-average and spin-dependent lepton and hadron tensors (10), (24–26). The analyses of the leading over s contribution to the cross sections have been carried out with the help of the REDUCE and MAPLE programs. We summarize over the spin of the J/Ψ meson and use (33) in calculation. In both cases, the squared amplitude of the J/Ψ electroproduction is expressed through the integral over l, l':

$$|T^\pm|^2 = \int d^2 l_\perp d^2 l'_\perp D(t, Q^2, l_\perp) D(t, Q^2, l'_\perp) \cdot F^\pm[A(l_\perp), B(l_\perp); A^\star(l'_\perp), B^\star(l'_\perp)], \quad (37)$$

where the functions $F^\pm$ include the A and B amplitudes from (17). The l dependence of these functions for small l has been discussed in, e.g., the second reference of [9]. The function D is determined by the contribution of the t-channel gluon propagators and the sum of the $\gamma\mathbf{P} \to {\rm J}/\Psi$ transition amplitude (32) for the graphs of Fig. 1a,b:

$$D(t, Q^2, l_\perp) = \frac{1}{(l^2_\perp + \lambda^2)((\mathbf{l}_\perp + \mathbf{r}_\perp)^2 + \lambda^2)} \cdot \left(\frac{n_a}{r^2 - m_{\rm c}^2} + \frac{n_b}{w^2 - m_{\rm c}^2}\right). \quad (38)$$

The leading-order s terms in the numerators $n_{a(b)}$ for the graphs, Fig. 1a,b, have a similar form but are different in sign: $n_b \sim -n_a = n$. In the sum of diagrams, Fig. 1a,b, their contributions mainly compensate for each other:

$$\frac{n}{w^2 - m_{\rm c}^2} - \frac{n}{r^2 - m_{\rm c}^2} = \frac{2n(l^2_\perp + \mathbf{l}_\perp \mathbf{r}_\perp)}{(M^2_{\rm J} + Q^2 + |t|)\,[l^2_\perp + \mathbf{l}_\perp \mathbf{r}_\perp + (M^2_{\rm J} + Q^2 + |t|)/4]}. \quad (39)$$

This function determines the Q^2 dependence of D. It can be seen that the typical scale in the integral (37) is defined by (39) and is of the order $\bar{l}^2_\perp \sim (M^2_{\rm J} + Q^2 + |t|)/4$ [10,11]. As a result, (37) can be estimated in the form

$$|T^\pm|^2 = F^\pm(A, B; A^\star, B^\star) I^2;$$
$$I = \int {\rm d}^2 l_\perp D(t, Q^2, l_\perp). \quad (40)$$

The functions A and B in $F^\pm$ are dependent on the scale

$$\bar{l}^2_\perp \sim \bar{Q}^2 = (M^2_{\rm J} + Q^2 + |t|)/4. \quad (41)$$

The cross section of the J/Ψ leptoproduction can be written in the form

$$\frac{{\rm d}\sigma^\pm}{{\rm d}Q^2 {\rm d}y {\rm d}t} = \frac{|T^\pm|^2}{32(2\pi)^3 Q^2 s^2 y}. \quad (42)$$

For the spin-average squared amplitude, we find

$$|T^+|^2 = N((2 - 2y + y^2)m^2_{\rm J} + 2(1 - y)Q^2)s^2 \cdot [|B + 2mA|^2 + |A|^2|t|]I^2. \quad (43)$$

Here N is a normalization factor:

$$N = \frac{\Gamma^{\rm J}_{\rm e^+e^-} M_{\rm J} \alpha_s^4}{27\pi^2}. \quad (44)$$

In (43), the term proportional to $(2-2y+y^2)m_{\rm J}^2$ represents the contribution of a virtual photon with transverse polarization. The $2(1-y)Q^2$ term describes the effect of longitudinal photons. Thus, we see that the ratio of $\sigma_{\rm T}/\sigma_{\rm L} \propto m_{\rm J}^2/Q^2$. Such behavior is typical of a simple form of the vector-meson wave function used here (see, e.g., [28])

The spin-dependent squared amplitude looks like

$$|T^-|^2 = N(2-y)s|t|[|B|^2 + m(A^\star B + AB^\star)]m_{\rm J}^2 I^2. \quad (45)$$

We find that $|T^-|^2$ vanishes in the forward direction ($t=0$) and is suppressed as a power of s with respect to (43). The reason for this suppression is quite simple. The leading contribution to $\sigma(-)$ is from the term $\epsilon^{\alpha\beta\gamma\rho}(r_{\rm P})_\gamma \ldots$, which is proportional to $x_{\rm P}p$. As a result, an additional $x_{\rm p}$ appears in $\sigma(-)$. This has been confirmed by the calculation of the $A_{\rm ll}$ asymmetry in different diffractive reactions [18,29]. In the case of vector-meson production, $x_{\rm P}$ is small (7) and behaves like $1/s$. Hence, longitudinal double-spin asymmetry in this diffractive process will be small at high energies; this is confirmed by our calculations for (45) and (43).

5 Numerical results for spin-dependent cross sections

We shall calculate the polarized cross section of the diffractive J/Ψ production (42) for the amplitudes (43, 45). The connection of the spin-average cross section of the J/Ψ production with the gluon distribution function is known as [10,11]

$$\left.\frac{{\rm d}\sigma}{{\rm d}t}\right|_{t\sim 0} \propto F_B^2(t)\left(x_{\rm P}G(x_{\rm P},\bar{Q}^2)\right)^2. \quad (46)$$

Here $F_B(t)$ is a new form factor which describes the t dependence of the two-gluon coupling with the proton. The expression of this cross section through the Pomeron–proton structure has been found in (43). It can be seen that the B function in (17) can be written as a product of the form factor and the gluon distribution

$$B(t,x_{\rm P},\bar{Q}^2) = F_B(t)\left(x_{\rm P}G(x_{\rm P},\bar{Q}^2)\right). \quad (47)$$

As the Pomeron–proton vertex might be similar to the photon–proton coupling [8], we shall use a simple approximation,

$$F_B(t) \sim F_{\rm p}^{\rm em}(t), \quad (48)$$

where $F_{\rm p}^{\rm em}(t)$ is the standard form for the electromagnetic form factor of the proton

$$F_{\rm p}^{\rm em}(t) = \frac{(4m_{\rm p}^2 + 2.8|t|)}{(4m_{\rm p}^2+|t|)(1+|t|/0.7\ {\rm GeV}^2)^2}. \quad (49)$$

It has been shown in (43, 45) that the leading contributions to the T^+ and T^- amplitudes are determined by the same loop integral I. For simplicity, we shall suppose that the A amplitude can be parameterized in a form similar to (47):

$$A(t,x_{\rm P},\bar{Q}^2) = \alpha F_A(t)\left(x_{\rm P}G(x_{\rm P},\bar{Q}^2)\right). \quad (50)$$

As above, the new form factor $F_A(t)$ describes the t dependence of the two-gluon coupling with the proton for the A function. We shall use for simplicity $F_A = F_{\rm p}^{\rm em}$. For the approximation (50), the ratio of the A and B amplitudes is independent of x. The $\alpha = A/B$ ratio determines through the x dependencies of the functions ($x \sim 1/s$ in this case) the energy behavior of the spin asymmetries in exclusive reactions at high energies and fixed momentum transfer. Thus, (47) and (50) result in energy independence of spin asymmetries which is in agreement with their weak energy dependence obtained in the models [22,23,25]. To study the α sensitivity of the cross section, we shall use in our estimations the value $|\alpha| \le 0.1\ {\rm GeV}^{-1}$. It has been mentioned above that this magnitude is consistent with the model estimations [22,23].

The energy dependence of the cross sections is determined by the Pomeron contribution to the gluon distribution function at small x:

$$\left(x_{\rm P}G(x_{\rm P},\bar{Q}^2)\right) \sim \left(\frac{sy}{m_{\rm J}^2+Q^2+|t|}\right)^{(\alpha_{\rm p}(t)-1)}. \quad (51)$$

Here $\alpha_{\rm p}(t)$ is a Pomeron trajectory. The linear approximation of the Pomeron trajectory (1) is used. The parameters of this trajectory were determined from the fit of the diffractive J/Ψ production by ZEUS [30]:

$$\alpha_{\rm p}(t) = 1 + (0.175 \pm 0.026) + (0.015 \pm 0.065)t. \quad (52)$$

In our model estimations of the polarized cross section of the diffractive J/Ψ production, we shall use the values $\epsilon = 0.15$ and $\alpha' = 0$, which are not far from (52). The typical scale of the reaction is determined by (41). For non-large Q^2 and $|t|$, the value of $\bar{Q}^2$ is about 2.5–3.0 GeV^2. In this region, we can work with fixed $\alpha_s \sim 0.3$. An effective gluon mass in (38) is chosen to be equal to 0.3 GeV^2. The cross section depends weakly on this parameter. The value of $\Gamma^{\rm J}_{\rm e^+e^-} = 5.26$ keV is used.

We integrate the cross sections (42) over Q^2 and y to get the differential cross sections of the J/Ψ production:

$$\frac{{\rm d}\sigma^\pm}{{\rm d}t} = \int_{y_{\min}}^{y_{\max}} {\rm d}y \int_{Q^2_{\min}}^{Q^2_{\max}} {\rm d}Q^2 \frac{{\rm d}\sigma^\pm}{{\rm d}Q^2{\rm d}y{\rm d}t}, \quad (53)$$

where

$$Q^2_{\min} = m_e^2 \frac{y^2}{1-y} \ \text{ and } \ Q^2_{\max} = 4\ {\rm Gev}^2.$$

For the HERA energy $\sqrt{s} = 300$ GeV, we integrate over the energy in the photon–proton system 30 GeV $< W_{\gamma{\rm p}} <$ 150 GeV ($W_{\gamma{\rm p}} \sim \sqrt{ys}$), which is equivalent to

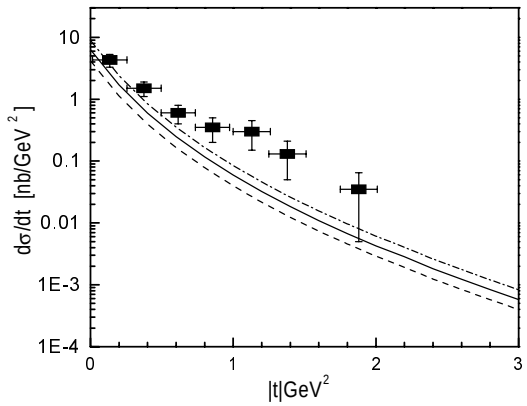

Fig. 2. The differential cross section of the J/Ψ production at HERA energy. Solid line: $\alpha = 0$; dot–dashed line: $\alpha = 0.1$ GeV^{-1}; dashed line: $\alpha = -0.1$ GeV^{-1}. Data are from [3]

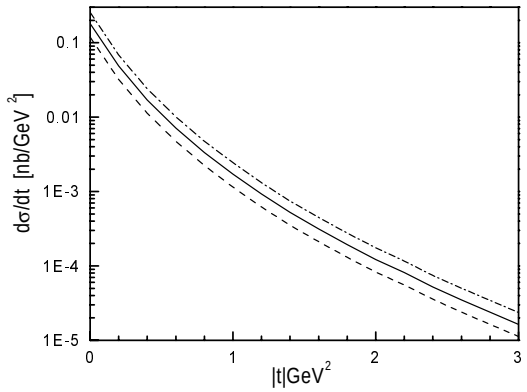

Fig. 3. The differential cross section of the J/Ψ production at HERMES energy. Solid line: $\alpha = 0$; dot–dashed line: $\alpha = 0.1$ GeV^{-1}; dashed line: $\alpha = -0.1$ GeV^{-1}

the range $0.01 < y < 0.25$. Our results, shown in Fig. 2, describe experimental data [3] at small $|t|$ and lie a little below them for momentum transfer larger than 1 GeV^2. This may indicate that the simple approximation of the form factor (48) used here is not good for $|t| > 1$ GeV^2. Our estimation for the HERMES energy $s = 50$ GeV^2 is performed for integration over $0.3 < y < 0.7$. The predicted cross sections are shown in Fig. 3. It is seen from Figs. 2 and 3 that the spin-average cross sections are sensitive to α, but the shape of all curves are the same. Thus, it is difficult to extract information about the spin-dependent part of the Pomeron coupling from the spin-average cross section of the diffractive vector-meson production.

Using the same formulas, we calculate the cross section $\sigma(-)$. This gives us a possibility for estimating the longitudinal double-spin A_{ll} asymmetry of the J/Ψ production at high energies. As has been found, the asymmetry vanishes as $1/s$, and for the HERA energy range, the expected value of A_{ll} will be negligible. The predicted asymmetry for HERMES as a function of α is shown in Fig. 4. The important property of A_{ll} is that the asymmetry of the vector-meson production is equal to zero in the

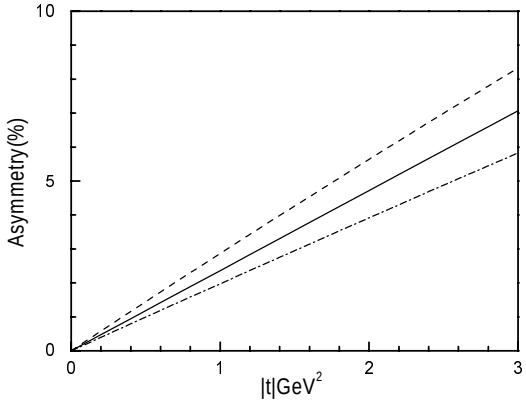

Fig. 4. The predicted A_{ll} asymmetry of the J/Ψ production at HERMES. Solid line: $\alpha = 0$; dot–dashed line: $\alpha = 0.1$ GeV^{-1}; dashed line: $\alpha = -0.1$ GeV^{-1}

forward direction. The A_{ll} asymmetry might be connected with the spin-dependent gluon distribution ΔG only for $|t| = 0$. Thus, ΔG cannot be extracted from A_{ll}; this is in agreement with the results of [17].

To understand the α dependence of the asymmetry, we shall use the approximated expression of the integral (53). The functions $\mathrm{d}\sigma^{\pm}/(\mathrm{d}Q^2\mathrm{d}y\mathrm{d}t)$ decrease very rapidly with growing Q^2. Calculating only the leading log terms of the integral over Q^2 in (53), we can write the double-spin asymmetry A_{ll} in the simple form

$$A_{ll} \sim \frac{|t|}{s} \frac{(2-\bar{y})(1+2m\alpha)}{(2-2\bar{y}+\bar{y}^2)\left[(1+2m\alpha)^2+\alpha^2|t|\right]}, \qquad (54)$$

where $\bar{y}$ is some average value in the integration region. We find that the asymmetry is nonzero for $\alpha = 0$:

$$A_{ll}^0 = A_{ll}(\alpha = 0) \simeq \frac{|t|}{s} \frac{(2-\bar{y})}{(2-2\bar{y}+\bar{y}^2)}. \qquad (55)$$

This asymmetry term is determined by the ΔA_γ contribution to $W(-)$ (see (27)). Both spin-average and spin-dependent cross sections (43, 45) are proportional to $|B|^2 \sim \left(x_{\mathrm{P}} G(x_{\mathrm{P}}, \bar{Q}^2)\right)$ for $\alpha = 0$, which results in the independence of A_{ll}^0 on the gluon distribution. We see from Fig. 4 that the A_{ll}^0 part of the asymmetry dominates. The value of the asymmetry for $\alpha \neq 0$ is determined by the spin-dependent part of the Pomeron coupling. However, the sensitivity of the asymmetry to α is not very strong. Thus, it will not be so easy to study the spin structure of the Pomeron coupling with the proton from the A_{ll} asymmetry of the diffractive J/Ψ production.

6 Conclusion

In the present paper, the polarized cross section of the diffractive J/Ψ leptoproduction at high energies has been studied. The relevant cross section can be determined in terms of the leptonic and hadronic tensors and the squared amplitude of the vector-meson production, through the photon–Pomeron fusion. The amplitude of the $\gamma\mathbb{P} \to \mathrm{J}/\Psi$

transition is described by the simple nonrelativistic wave function. This approximation is efficient, at least for heavy-meson production. The introduced hadronic tensor is expressed in terms of the Pomeron–proton coupling structure which has the helicity-flip part. As a result, a connection between the spin-dependent cross section in the diffractive J/Ψ production and the Pomeron coupling has been found. We predict a nonsmall value of the A_{ll} asymmetry of the diffractive vector-meson production at the HERMES energy. However, the asymmetry decreases as $1/s$ with growing energy, and at the HERA energy, it will be extremely small. It has been found that the A_{ll} asymmetry vanishes at $t = 0$. Thus, it is impossible to extract the polarized gluon distribution ΔG from the asymmetry. The predicted asymmetry is independent of the mass of a produced meson. We can expect a similar value of the asymmetry in the polarized diffractive ϕ–meson leptoproduction.

Our results show the essential role of the γ-coupling asymmetry in A_{ll}. In this case the asymmetry does not vanish for nonzero $|t|$ and is completely determined by the γ^{α} term in the Pomeron coupling (13, 17). It does not depend on the gluon distribution and appears to exhibit a kinematic character. This form of the Pomeron coupling is typical of the QCD-based models of the Pomeron [13–15, 20]. Note that the soft Pomeron model leads to zero A_{ll} asymmetry in the hadronic leptoproduction [31].

The longitudinal double-spin asymmetry of the vector-meson production for nonzero momentum transfer has been found to be dependent on the A term of the Pomeron coupling, which produces helicity-flip effects. Note that this spin-dependent part of the coupling A is parametrized here by the gluon structure function of the proton G for simplicity. Generally, the function A should be determined by the polarized gluon distribution, and the ratio α might depend on x_{P} and t. However, this conformity is not very well known now. To find the explicit connection of A with spin-dependent gluon distribution in QCD, additional study is necessary. The information about the spin structure of the Pomeron coupling can generally be extracted from the A_{ll} asymmetry of the vector-meson production for $|t| \neq 0$. Such investigations can be carried out in future polarized experiments at CERN and DESY. However, the sensitivity of asymmetry to the α ratio is quite weak. Thus, the diffractive vector meson production might not be a good tool to study the polarized gluon distributions of the proton or the spin structure of the Pomeron.

Acknowledgements. We would like to thank A. De Roeck, A. Efremov, P. Kroll, T. Morii, O. Nachtmann, W.-D. Nowak, M. Ryskin, and O. Teryaev for fruitful discussions. This work was supported in part by the Heisenberg–Landau Grant.

References

1. H1 Collaboration: T. Ahmed, et al., Phys. Lett. B **348**, 681 (1995); ZEUS Collaboration: M. Derrick, et al., Z. Phys. C **68**, 569 (1995)
2. ZEUS Collaboration: M. Derrick, et al., Z. Phys. C **70**, 391 (1996); H1 Collaboration: C. Adloff, et al., Z. Phys. C **76**, 613 (1997)
3. H1 Collaboration: S. Aid, et al., Nucl. Phys. B **472**, 3 (1996)
4. ZEUS Collaboration: J. Breitweg, et al., Z. Phys. C **75**, 215 (1997); HERMES Collaboration: M. Düren, et al., to appear in *Proceedings of LISHEP 98, Workshop on Diffractive Physics, Rio de Janeiro, February 1998*
5. A. Donnachie and P.V. Landshoff, Nucl. Phys. B **267**, 690 (1986);
6. S.V. Goloskokov, S.P. Kuleshov, and O.V. Selyugin, Mod. Phys. Lett. A **10**, 1959 (1995)
7. E.A. Kuraev, L.N. Lipatov, and V.S. Fadin, Sov. Phys. JETP. **44**, 443 (1976); P.V. Landshoff and O. Nachtmann, Z. Phys. C **35**, 405 (1987)
8. A. Donnachie and P.V. Landshoff, Nucl. Phys. B **311**, 509 (1989); A. Schäfer, L. Mankiewicz, and O. Nachtmann, Phys. Lett. B **272**, 419 (1991)
9. J.R. Cudell, Nucl. Phys. B **336**, 1 (1990); J.R. Cudell and I. Royen, Phys. Lett. B **397**, 317 (1997)
10. M.G. Ryskin, Z. Phys. C **57**, 89 (1993)
11. S.J. Brodsky, et al., Phys. Rev. D **50**, 3134 (1994)
12. F.E. Low, Phys. Rev. D **12**, 163 (1975); S. Nussinov, Phys. Rev. Lett. **34**, 1286 (1975)
13. A. Donnachie and P.V. Landshoff, Nucl. Phys. B **244**, 322 (1984)
14. T. Arens, M. Diehl, O. Nachtmann, and P.V. Landshoff, Z. Phys. C **74**, 651 (1997)
15. J. Klenner, A. Schafer, and W. Greiner, Z. Phys. A **352**, 203 (1995)
16. M.G. Ryskin, Phys. Lett. B **403**, 335 (1997)
17. M. Vänttinen and L. Mankiewicz, Phys. Lett. B **434**, 141 (1998)
18. S.V. Goloskokov, e-print: hep-ph/9809577, hep-ph/9811450
19. M. Diehl, Eur. Phys. J. C **4**, 497 (1998)
20. P.V. Landshoff and O. Nachtmann, Z. Phys. C **35**, 405 (1987)
21. M. Anselmino, A. Efremov, and E. Leader, Phys. Rept. **261**, 1 (1995)
22. S.V. Goloskokov, S.P. Kuleshov, and O.V. Selyugin, Z. Phys. C **50**, 455 (1991)
23. S.V. Goloskokov and P. Kroll, Phys.Rev. D **60**, 014019 (1999)
24. N. Akchurin, N.H. Buttimore, and A. Penzo, Phys. Rev. D **51**, 3944 (1995)
25. C. Bourrely, J. Soffer, and T.T. Wu, Phys. Rev. D **19**, 3249 (1979)
26. M. Anselmino, P. Kroll, and B. Pire, Z. Phys. C **36**, 89 (1987)
27. E.L. Berger and D. Jones, Phys. Rev. D **23**, 1521 (1981)
28. I. Royen, J.R. Cudell, e-print: hep-ph/9807294
29. S.V. Goloskokov, Mod. Phys. Lett. **12**, 173 (1997)
30. ZEUS Collaboration: "Study of vector-meson production at large $|t|$ at HERA and determination of the Pomeron trajectory", to appear in *Proceedings of the XXIX International Conference on High Energy Phys., Vancouver, July, 1998*
31. S.I. Manayenkov, e-print: hep-ph/9903405